High Power SiC Modules for HEVs and PHEVs

M. Chinthavali[1], L. M. Tolbert[1], H. Zhang[2], J. H. Han[3], F.Barlow[4], B. Ozpineci[1]

[1]Power Electronics and Electric Machinery Research Center Oak Ridge National Laboratory, Knoxville, TN 37932
[2]Electrical Engineering Department Tuskegee University Tuskegee, Al 36088
[3]Global Power Electronics 27, Mauchly Ste 206, Irvine, CA 92618
[4]Electrical and Computer Engineering University of Idaho Moscow, Idaho 83844-1023

***Abstract*—With efforts to reduce the cost, size, and thermal management systems for the power electronics drivetrain in hybrid electric vehicles (HEVs) and plug-in hybrid electric vehicles (PHEVs), wide band gap semiconductors including silicon carbide (SiC) have been identified as possibly being a partial solution. Research on SiC power electronics has shown their higher efficiency compared to Si power electronics due to significantly lower conduction and switching losses. This paper focuses on the development of a high power module based on SiC JFETs and Schottky diodes. Characterization of a single device, a module developed using the same device, and finally an inverter built using the modules is presented. When tested at moderate load levels compared to the inverter rating, an efficiency of 98.2% was achieved by the initial prototype.**

***Index Terms*—Silicon Carbide, JFET, inverter, efficiency, hybrid electric vehicle, HEV, PHEV.**

I. Introduction

Development of power electronics and electric machine technology will be the key to the U.S. Department of Energy's (DOE) mission to reduce energy dependency on oil for transportation. The objective of DOE's advanced power electronics and electric machinery (APEEM) activity is to develop technology towards achieving overall electric propulsion system targets for year 2015 and 2020 as shown in Table I for hybrid electric vehicles (HEVs). The drive system is expected to last for 15 years and to operate at 55 kW peak power for 18 seconds and at 30 kW continuous power rating. The efficiencies shown in Table I are at 20 % of rated torque and over the 10 - 100% speed range. The targets are based on a liquid coolant temperature of 105 °C. The overall targets were further divided for inverter and motor specific targets as shown in Table II [1].

In present HEVs, the traction drive including the power electronics and motor make up more than 50% of the traction drive system cost, with the batteries and electric generator accounting for less than 50% of the cost. Thus, most of the effort is focused on reducing these costs while at the same time minimizing the volume and weight of these components.

[1]Prepared by the Oak Ridge National Laboratory, Oak Ridge, Tennessee 37831, managed by UT-Battelle for the U.S. Department of Energy under contract DE-AC05-00OR22725.

Plug-in hybrid electric vehicle (PHEV) cost targets for the APEEM as established by DOE for PHEVs with all-electric range capabilities is $1680 (U.S. $). Present PHEV PEEM systems cost almost three times this amount. For PHEVs without all-electric range capability the cost goal is $840, which is also almost three times less than present costs.

Integration of the drive system is very important to meet the specific power and volumetric goals. Present hybrid electric vehicles typically have two coolant loops: (1) one for the engine at 105 °C, and (2) a separate one for the power electronics and traction motor at 65 – 70 °C. Research in eliminating the low temperature loop and using the engine coolant for the APEEM shows that it would be quite difficult to use the present silicon-based power electronics.

Another option is to replace the liquid cooled systems for the PEEM with air-cooled systems because this will reduce the complexity of system integration and reduce the cost by eliminating the additional cooling loop in the existing hybrid vehicles. However, this requires reliable operation of all the components in the drive system in an under-the-hood high temperature environment.

Development of new power devices is a critical aspect for future power electronic applications along with new topologies and control techniques. The semiconductor device industry has been aggressively pursuing the development of high temperature wide bandgap (WBG) devices for more than a decade to cater to the need for high temperature applications. There is a revolutionary change in the power electronics WBG devices making inroads into the power semiconductor device market.

TABLE I. Traction Drive Targets

Traction Drive System				
Year	($/kW)	(kW/kg)	(kW/l)	Efficiency
2015	12	1.2	3.5	>93%
2020	8	1.4	4	>94%

TABLE II. Motor and Inverter Targets

	Inverter			Motor		
Year	($/kW)	(kW/kg)	(kW/l)	($/kW)	(kW/kg)	(kW/l)
2015	5	12	12	7	1.3	5
2020	3.3	14.1	13.4	4.7	1.6	5.7

SiC is the frontrunner amongst the WBG material based devices. Silicon carbide power devices are expected to replace the silicon (Si) devices in high-voltage, high-temperature, and high-frequency applications because of the system level benefits that can be realized when using SiC devices. SiC Schottky diodes have now been commercially available for almost 10 years. To date, SiC controllable switches, however, have only been available as engineering samples.

The device level development of SiC has progressed from designing discrete level low amperage devices to building modules with scalable devices and higher power ratings. This growth has enabled researchers to test modules for efficiency comparison with silicon devices and also build several converter and inverter prototypes. SiC discrete devices have been compared with Si devices showing the benefits of SiC devices in many publications [2-4, 9-10].

High temperature packaging was recognized as a necessary area to be developed in parallel with development of SiC technology, so that the benefits of the SiC devices can be more fully realized in many applications. WBG research at Oak Ridge National Laboratory is focused on the development of highly efficient, high temperature SiC based inverters for automotive and power system applications. Research involves work on high temperature packaging (>200°C), high temperature gate drive electronics that can work at 200°C [5], inverter design and prototype development, efficiency estimation with device and system simulation, and experimental characterization.

High power SiC modules have been built and their performance has been evaluated as reported in [6-9]. Just by exchanging the silicon freewheeling diodes with silicon carbide Schottky diodes, the losses in the traction drive would be reduced by 10 - 30 % in a 55 kW inverter that had Si IGBTs and was designed for HEV traction applications [9].

This paper presents characterization of a SiC JFET as a discrete device and paralleled in a half bridge module. The discrete device presented in this paper is a normally-on 1200 V, 10 A SiC JFET (specific resistance = 150 mΩ). The devices in modules that were characterized are SiC JFETs and Schottky diodes in a 1200 V, 30 A high temperature packaged module. Finally, the test results of an 18 kW all-SiC inverter prototype built using modules with SiC JFETs and SiC Schottky diodes will be presented.

II. Design and Development of SiC Module

A SiC JFET-based phase leg module with hermetic metal housing was developed as shown in Fig. 1(a). The package is designed to work at a temperature of at least 200 ºC ambient. Each module is a single phase leg with six 1200 V SiC JFETs (normally-on) and two 1200 V Schottky diodes from SiCED as well as a thermistor to detect the temperature inside the module (see Fig. 1(b)). Three SiC JFETs were paralleled in order to achieve a higher current rating (~30A).

The packages were built based on hermetic metallic housings and direct bond copper (DBC) substrates as shown in

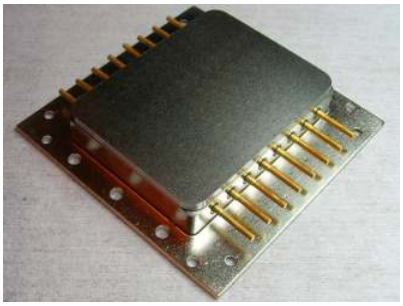

(a) CTE-matched metal lid and housing.

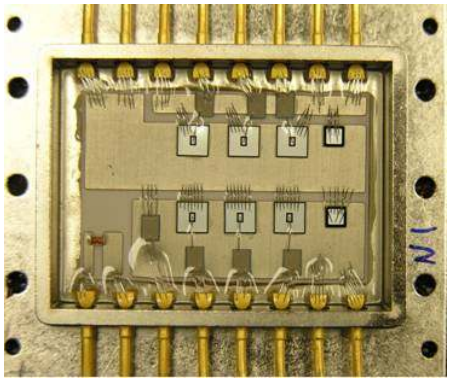

(b) Six SiC JFETs and two SiC Schottky diodes are attached to substrate and are wire bonded with aluminum alloy wire.

Fig. 1. SiC JFET phase leg module with hermetic metal housing.

Fig. 2. Metal housings were selected due to the high reliability associated with these packages even at temperatures well above 200 °C. The use of coefficient of thermal expansion (CTE) matched metals, and glass isolated electrical connections ensures thermal and mechanical stability far superior to traditional plastic modules.

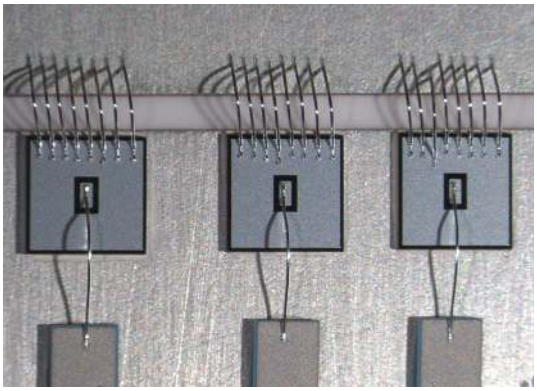

Fig. 2. SiC JFETs bonded to a DBC BeO substrate within the power module's housing.

Each individual module contains a single DBC substrate that is used to interconnect the SiC-based diodes and JFETs. Beryllium oxide (BeO) was chosen for the substrate in this application due to its superior thermal performance, but versions of this module could also be fabricated with Alumina (Al_2O_3) or Aluminum Nitride (AlN) substrates, with slightly

lower thermal performance [11-14]. The SiC devices were attached to these substrates through the use of a polyimide based conductive adhesive. This adhesive is stable to well above 200 °C and therefore can be used when many of the traditional solders would melt.

The SiC devices were then wire bonded with aluminum alloy wire to form the connections between the die, substrate traces, and external electrical connections. In modules of this nature, the metallization must be carefully considered to avoid failures caused by inter-metallic alloy formation at the die wire bond interface, or the substrate wire bond interface. If selected inappropriately, inter-diffusion, which is accelerated at high temperatures, can lead to void formation and a reduction in the strength of the bond welds.

The most famous case is the Al / Au inter-metallic bonding [15] but similar effects have been observed in the Al / Cu system [16]. In this case, a surface finish of Nickel was selected since it has been established that the Ni / Al system is far more stable at high temperatures than many of the alternative systems [17-19].

After assembly of the modules, a low modulus encapsulation was used to suppress arcing in and around the die and wire bonds within the metal housings. This material is applied in a liquid state and therefore flows around the structures within the module. Once cured, it becomes a soft rubber like material that is stable to temperatures up to 200 °C. A detailed analysis of this material indicates no change in the breakdown voltage even after more than 1000 hours of exposure to high temperatures. Finally, a CTE matched metal lid was sealed in place.

III. Comparison of Discrete Devices and Module

A. Static Characteristics

Forward characteristics of a discrete (1200 V, 10 A) SiC JFET are shown in Fig. 3 for different operating temperatures from 25°C to 175°C in 25°C increments. SiC JFETs exhibit linear relationship between the voltage and current and can be modeled as a resistor. The resistive component has a positive temperature coefficient which means their conduction losses will be higher at higher temperatures. However, a positive temperature coefficient makes it easier to parallel these devices and reduce the overall on-resistance. The forward characteristics of the paralleled SiC JFETs in the module are shown in Fig. 4 for operating temperatures from 25 °C to 200 °C in 25°C increments.

The linearity of the curves seen in the discrete device characteristics is still preserved after paralleling devices. The on-state resistance was extracted from the forward characteristic curves at different temperatures and is shown in Fig. 5. A comparison of the on-resistance between the single device and paralleled devices shows that the devices scale linearly by almost a factor of three over a wide range of temperature from 25 °C to 200 °C.

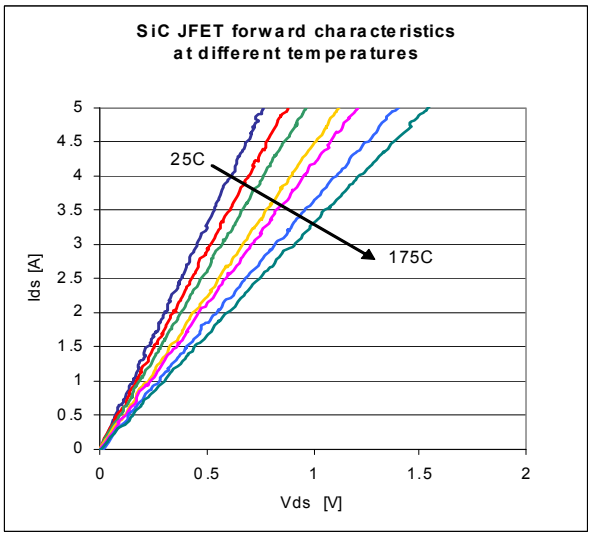

Fig. 3. Forward characteristics of normally-on SiC JFET.

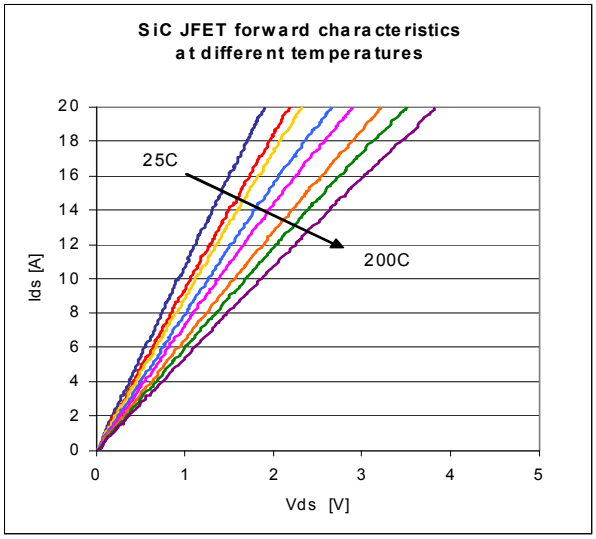

Fig. 4. Forward characteristics of three paralleled normally-on SiC JFETs in module.

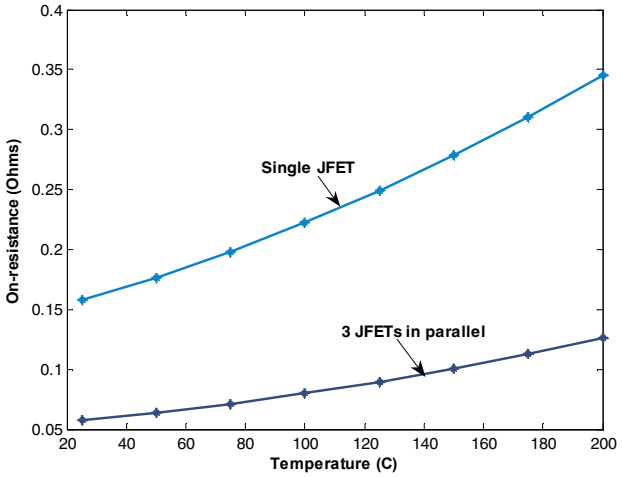

Fig. 5. On-resistance of single JFET and three paralleled JFETs.

The transfer characteristics of the single discrete device at different temperatures show the pinch-off voltage does not change with temperature over temperature range from 25°C to 175°C as shown in Fig. 6. The transfer characteristics of the module as shown in Fig. 7 are also nearly constant for tested temperatures from 25°C to 200°C. However, it should be noted that the pinch-off voltage for the module JFETs is higher compared to the single device. The shift in the pinch-off voltage could be because of the difference in the device samples used in the module and the single device sample tested.

B. Dynamic Characteristics

Applying a sufficient negative voltage can turn off normally-on devices. Based on the transfer characteristics, a gate voltage swing of (0 V to −16 V) was selected since that would be enough to turn off most of the device samples tested. The peak gate current was about 0.5 A when using a gate resistance of 10 Ω [20]. The dynamic characteristics of the JFET were obtained using a double pulse circuit test at several temperatures and currents. The total energy losses of the JFET during switching are shown in Fig. 8. The total energy losses increase with current and do not change much with temperature (actually decrease slightly). The device losses were obtained at 200 V over a temperature range of 50 °C to 175 °C.

The switches (consisting of three paralleled JFETs) in the modules were also tested using a double pulse circuit for a temperature range of 50 ºC to 200 ºC with the increment of 50ºC. Commercial gate driver IC HCNW3120 was selected to drive the SiC JFETs. With proper design of power supply voltages, the gate driver IC can generate -20 V to turn off the JFETs, and 0 V for turn on. At 200ºC, the peak gate current for the module with three JFETs in parallel is about 1.6 A when using a gate resistance of 5 Ω which is triple the gate current required for single device.

The switching losses for the JFET module including both turn-on loss and turn-off loss for a voltage of 200 V are plotted

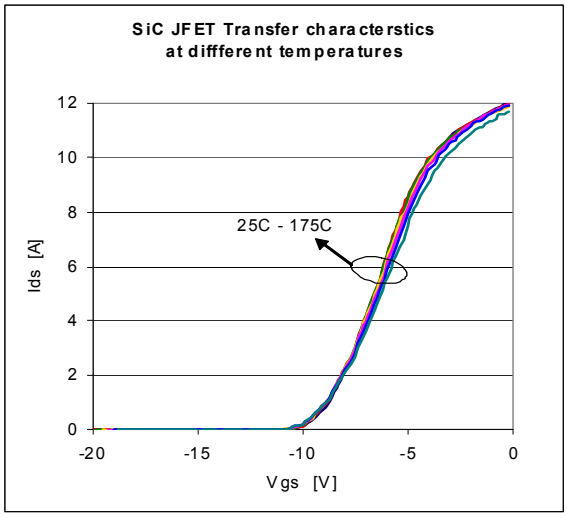

Fig. 6. Transfer characteristics of normally-on single SiC JFET at different temperatures.

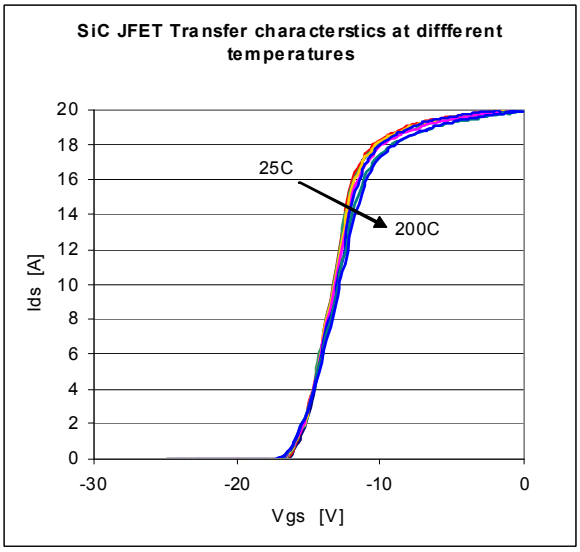

Fig. 7. Transfer characteristics of the paralleled SiC JFETs in the module at different temperatures.

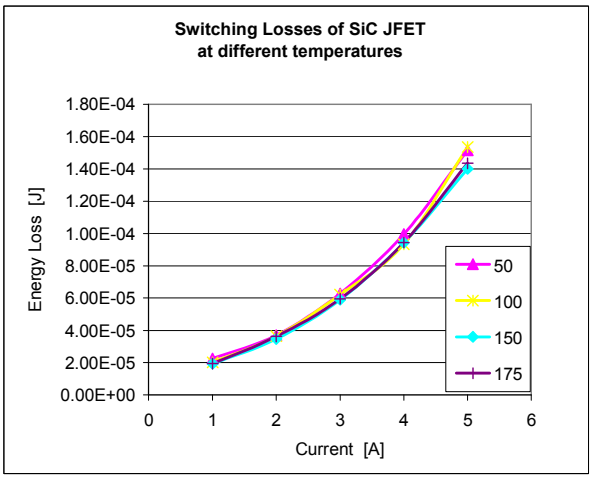

Fig. 8. Switching losses of a single normally-on JFET device.

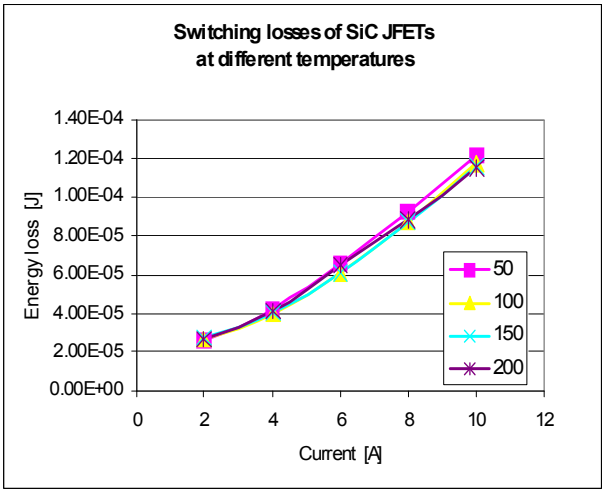

Fig. 9. Switching losses of three paralleled SiC JFETs in module.

versus the drain current at each tested temperature in Fig. 9. The switching losses in the SiC devices are almost constant (decrease only slightly) when temperature increases. The switching losses of the JFETs in the modules are approximately 1.5 times the losses for single device at three times the current.

IV. BODY DIODE OF A NORMALLY-ON SIC JFET

The body diode is only available in some normally-on JFETs and this particular JFET has a PiN diode formed because of the device design. The body diode could be used as the freewheeling diode in voltage source inverter based applications. By using this diode, the number of devices used in an inverter can be reduced by eliminating the anti-parallel diodes. However, the performance body diode needs to be evaluated so that it can replace the free-wheeling diode.

A. Static Characteristics

Static characteristics of the body diode in a 1200 V, 10 A SiC JFET for different operating temperatures are shown in Fig. 10. The on-state voltage is much higher than a similar rated Schottky diode [4]. This will make this diode inefficient at higher power levels

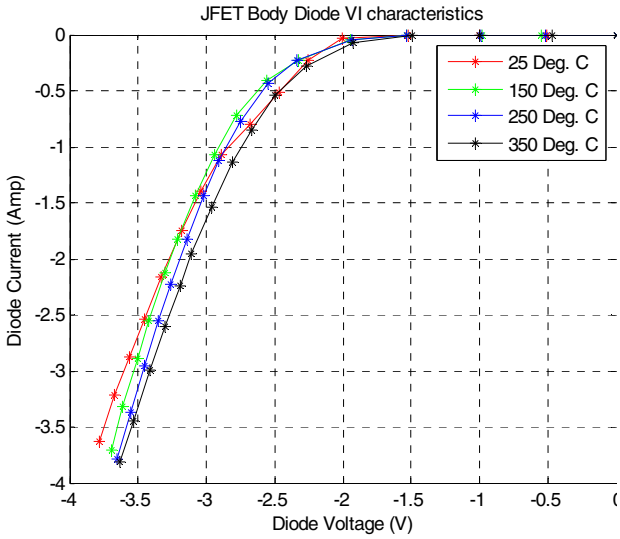

Fig. 10. Forward characteristics of body diode in a SiC JFET.

B. Dynamic Characteristics

The body diode has higher reverse recovery time unlike the zero recovery losses of the Schottky diode, which increases the switching losses of the inverter [4]. The reverse recovery characteristics of the body diode at different temperatures are shown in Fig. 11. The peak reverse recovery current increases with increase in temperature. However, the change in reverse recovery current is small resulting in minimal increase in reverse recovery losses at higher temperatures.

Based on the static and dynamic performance comparison of the body diode with the Schottky diode it can be concluded that body diode cannot be used.

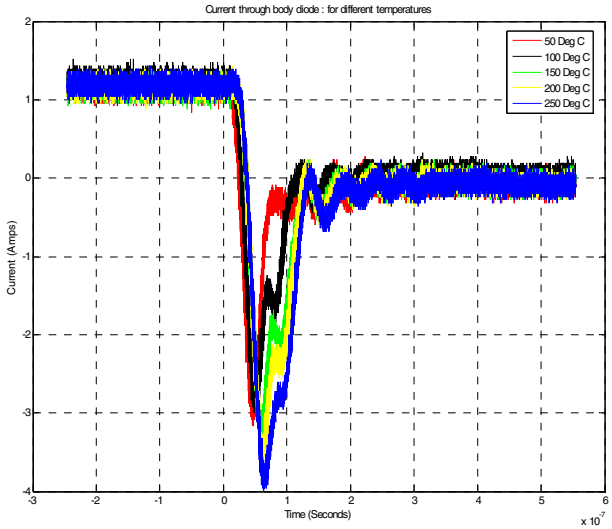

Fig. 11. Reverse recovery characteristics of body diode in a SiC JFET.

V. EXPERIMENTS AND SIC INVERTER EFFICIENCY

A SiC inverter was built using three SiC modules as shown in Fig. 12. The dimension of the inverter is 25 cm × 10 cm × 11 cm including the extruded heatsink and the control boards. The SiC inverter was tested with a 3-phase RL load, where R = 10 Ω and L =2 mH.

The switches in the inverter are controlled by SVPWM signals generated by the DSP board. The control program is developed in Matlab Simulink, and controllable parameters can be modified online. The input DC voltage and current and 3-phase output voltage and current are monitored and measured by oscilloscope and PZ4000. Some experimental waveforms of input voltage, output voltage, and output current are shown in Fig. 13. The input voltage in the figure is 500 V. The frequency of the output voltage is 60 Hz, and its magnitude is set by a modulation index of 0.85. As shown from Fig. 13(a)-(c), the

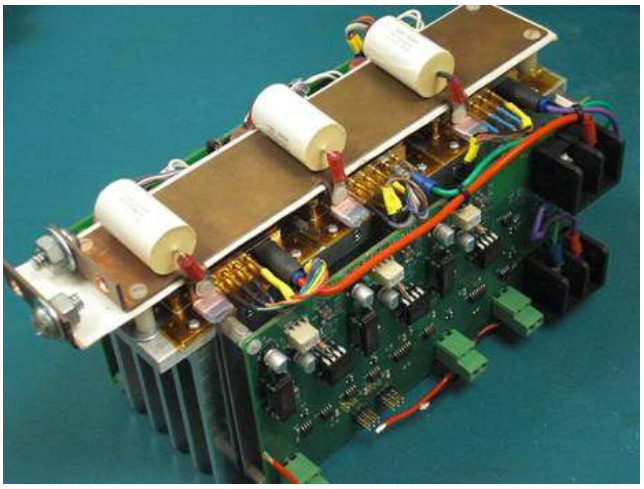

Fig. 12. Prototype SiC JFET inverter.

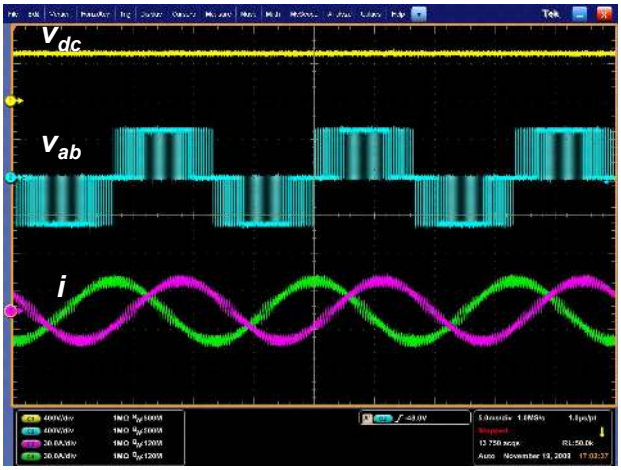

(a) at 5 kHz

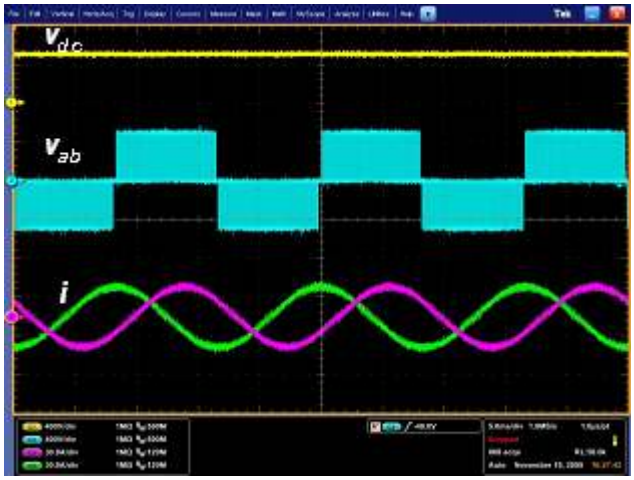

(b) at 10 kHz

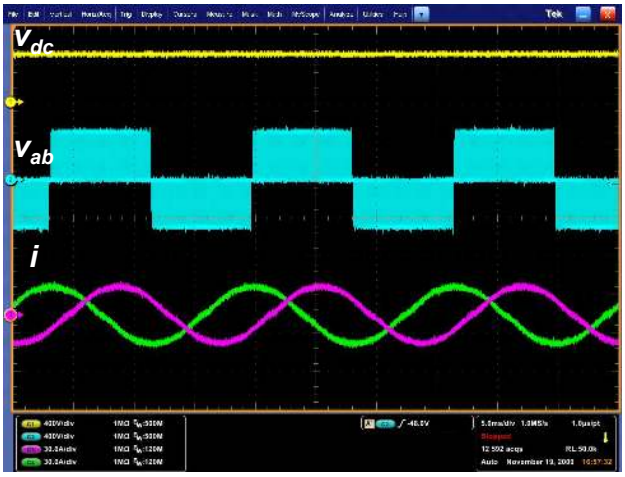

(c) at 20 kHz

Fig. 13. Experimental waveforms of the SiC inverter at 500 Vdc.

output current on the ac side is a clean sinusoidal waveform, and approaches to a fine sinusoidal waveform at increasing switching frequency.

The values of input and output current/voltage are recorded using PZ4000. The input power and output power are also calculated by PZ4000. The power loss and efficiency of the inverter can be calculated based on this information. Fig. 14 shows the inverter efficiencies at 60 Hz fundamental output frequency with a modulation index of 0.85 and three different switching frequencies (10, 15, 20 kHz). The maximum efficiency, 98.2%, is achieved at a switching frequency of 10 kHz at 4 kW output power range. The temperature inside the modules is less than 100 °C at this operating condition. Increasing the output power to more than 8 kW will cause the module temperatures to quickly increase as monitored by the thermistors inside the package. This indicates that the cooling capability of the present heatsink design is not enough for a power level more than 8 kW.

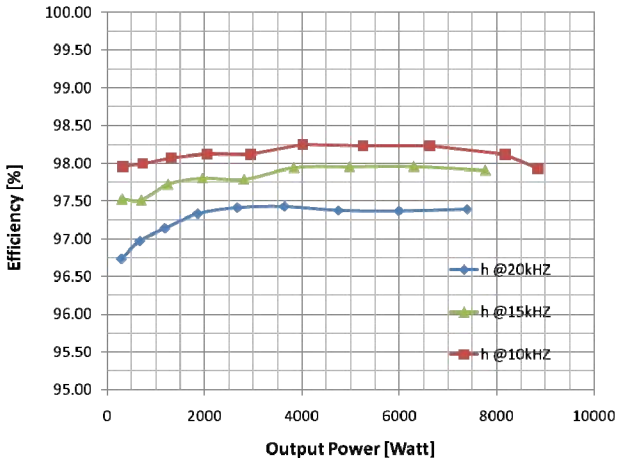

Fig. 14. Efficiency of the SiC inverter at different output power levels and switching frequencies.

VI. CONCLUSIONS

SiC phase-leg modules with high-temperature package (200 °C) are designed and demonstrated. Each switch inside the modules is composed of three SiC JFETs (1200 V / 10 A) in parallel. The test results of discrete devices and the devices in the modules were presented and discussed. The results gave an insight to the scaling of the devices for higher power modules.

A SiC inverter composed of three high temperature modules was developed and tested. The inverter efficiency at power levels up to 8 kW is better than 98% even with 10 kHz switching frequency. To fully utilize the device ratings and achieve better efficiency, the cooling capacity of present heatsink needs to be improved. This may involve further improving the packaging, optimizing the thermal management, and selecting high temperature passive components.

REFERENCES

[1] Freedom Car & Fuels Roadmap, November 2006. [Online]. Available: www1.eere.energy.gov/vehiclesandfuels/pdfs/program/eett_roadmap.pdf

[2] A. Elasser, T.P. Chow, "Silicon carbide benefits and advantages for power electronics circuits and systems," *Proceeding of IEEE*, vol. 90, no. 6, pp. 969-986, June 2002.

[3] A. R. Hefner, R. Singh, J. S. Lai, D. W. Berning, S. Bouche, and C. Chapuy, "SiC power diodes provide breakthrough performance for a wide range of applications," *IEEE Trans. Power Electronics*, vol. 16, pp. 273-280, Mar. 2001.

[4] L. M. Tolbert, H. Zhang, M. S. Chinthavali, B. Ozpineci, "SiC-based power converters for high temperature applications," *Materials Science Forum*, vols. 556-557, 2007, pp. 965-970.

[5] M. A Huque, L. M. Tolbert, B. J. Blalock, S. K. Islam, "A high-temperature, high-Voltage SOI gate driver IC with high output current and on-chip low-power temperature sensor," *IMAPS International Symposium on Microelectronics*, San Jose, California, Nov. 1-5, 2009, 8 pages.

[6] Y. Sugawara, D. Takayama, K. Asano, S. Ryu, A. Miyauchi, S. Ogata, and T. Hayashi, "4H-SiC high power SIJFET module," in *Proc. IEEE 15th International Symposium on Power Semiconductor Devices and ICs*, April 14-17, 2003, pp. 127 – 130.

[7] T. E. Salem, D. P. Urciuoli, R. Green, and G. K. Ovrebo, "High-temperature high-power operation of a 100 A SiC DMOSFET module," in *Proc. IEEE Applied Power Electronics Conference and Exposition*, Feb. 15-19, 2009, pp. 653 – 657.

[8] H. Zhang, M. Chinthavali, L. M. Tolbert, J. H. Han, F. Barlow, "18 kW three phase inverter system using hermetically sealed SiC phase-leg power modules," *IEEE Applied Power Electronics Conference*, Palm Springs, California, Feb. 21-25, 2010, pp. 1108-1112.

[9] B. Ozpineci, M. Chinthavali, A. Kashyap, L. M. Tolbert, A. Mantooth, "A 55 kW three-phase inverter with Si IGBTs and SiC Schottky diodes," *IEEE Transactions on Industry Applications*, vol. 45, no. 1, Jan./Feb. 2009, pp. 278-285.

[10] H. Zhang, L. M. Tolbert, B. Ozpineci, "Impact of SiC devices on hybrid electric and plug-in hybrid electric vehicles," *IEEE Industry Applications Society Annual Meeting*, Edmonton, Canada, October 5-9, 2008, 5 pages.

[11] M. A. Occhionero, R.W. Adams, and K. P. Fennessy, "A new substrate for electronic packaging: aluminum silicon carbide (AlSiC) composites," *Proceedings of the Forth Annual Portable by Design* Conference, Electronics Design, March 24–27, 1997, pp. 398-403.

[12] E. S. Dettmer, B. M. Romenesko, H. K. Charles, Jr., B. G. Carkhuff, and D. J. Merrill, "Steady-State thermal conductivity measurements of AlN and SiC substrate materials," IEEE Transactions on Components, Hybrids, and Manufacturing Technology, 12(4), December 1989, pp. 543-547.

[13] T. R. Bloom, "The reliability of AlN power hybrids using Cu thick film conductive," Proceedings of the 40th Electronic Components and Technology Conference, May 20–23, 1990, pp. 111-115.

[14] F. Barlow and A. Elshabini, "High-temperature high-power packaging techniques for HEV traction applications", ORNL/TM-2006/515, published by UT-Battelle, LLC, Oak Ridge National Laboratory, Oak Ridge, Tennessee, Nov. 2006.

[15] G. Harman, Wire bonding in microelectronics: materials, processes, reliability, and yield, Second Edition, McGraw-Hill Professional, June 1, 1997.

[16] D. Olsen, K. James, "Effects of ambient atmosphere on aluminum — copper wirebond reliability," IEEE Transactions on Hybrids and Manufacturing Technology, vol. 7, no. 4, December 1984, pp. 357-362.

[17] D. Palmer, "Hybrid microcircuitry for 300°C operation," IEEE Transactions on Parts, Hybrids, and Packaging, vol. 13, no. 3, September 1977, pp. 252-257.

[18] J. T. Benoit, S. Chin, R. R. Grzybowski, L. Shun-Tien, R. Jain, P. McCluskey, T. Bloom, "Wire bond metallurgy for high temperature electronics," pp. 109–113 in *High Temperature Electronics Fourth International Conference*, HITEC'98, June 14–18, 1998.

[19] J. T. Benoit, R. R. Grzybowski, D. B. Kerwin, "Evaluation of aluminum wire bonds for high temperature (2WC) electronic packaging," Transactions of the Third International High Temperature Electronics Conference, 1996, pp. III-17-23.

[20] H. Zhang, L. M. Tolbert, "Efficiency of SiC JFET-based inverters," The 4th IEEE Conference on Industry Electronics and Applications, May 25-27, 2009, Xi'an, China, pp. 2056-2059.